Robust Time-based Localization for Asynchronous Networks with Clock Offsets

Yiyin Wang *, Xiaoli Ma †, and Geert Leus *

*Faculty of Electrical Engineering, Delft University of Technology
Mekelweg 4, 2628CD Delft, The Netherlands
†School of Electrical and Computer Engineering, Georgia Institute of Technology
Atlanta, GA 30332-0250, USA

***Abstract*—Localization is indispensable for the successful deployment of wireless sensor networks (WSNs). Time-based localization approaches attract a lot of interest due to their high accuracy and potentially low cost. However, time-based localization is intensively coupled with clock synchronization. Thus, the reliability of timestamps in the time-based localization becomes an important yet challenging task to deal with. In this paper, we propose a robust time-based localization approach to locate a target node with the assistance of anchors (nodes with known positions) in an asynchronous network with clock offsets. We employ the asymmetric trip ranging (ATR) protocol to obtain time-of-arrival (TOA) measurements and facilitate clock offset cancellation. Regardless of the reliability of the timestamp report from the target node, closed-form least-squares (LS) and weighted LS estimators are derived to accurately estimate the target node position. As a result, we counter the uncertainties caused by the target node by ignoring the timestamps from this node. Furthermore, Cramér-Rao Bounds (CRBs) and simulation results corroborate the efficiency of our localization scheme.**

***Index Terms*—Localization, synchronization, clock offset, least squares, two-way ranging**

I. Introduction

Location-aware wireless sensor networks (WSNs) have attracted enormous interest from industry and academia due to their wide range of applications [1]. Location-awareness is crucial for the successful deployment of WSNs [2], [3]. The unique properties of ultra-wideband (UWB) impulse radio (IR) [2] facilitate localization based on time-of-arrival (TOA) or time-difference-of-arrival (TDOA) with high accuracy and potentially low cost [4]–[6]. As the TOA or TDOA measurements are time-based, clock synchronization [7] is tightly coupled with localization. However, localization and synchronization are traditionally treated as standalone problems, and only recently they have been jointly considered [8]–[13]. A preprocessor is first applied to cancel clock offsets, and then a maximum-likelihood (ML) estimator is derived to estimate all node positions in [8]. The two-way ranging (TWR) protocol proposed in the IEEE 802.15.4a standard [14] is employed in [9], [12] for asynchronous networks with not only clock offsets but also clock skews. In [9], the relative clock skews are first calibrated, and then the node positions are estimated in a distributed way. The internal delay is further considered in [12]. The impact of the clock skew is approximated as a zero mean random noise in [10], and intrasensor TDOAs are obtained by taking advantage of target motion, which also facilitates clock offset cancellation. However, it cannot be used to locate static target nodes. A localization approach based on triple-differences, which are the differences of two differential TDOAs, is proposed in [11], where the corrupted one-way TOA measurements due to the relative clock offset and clock skew are corrected by several steps. Two-way message exchanges are used in [13] for a scenario, where all the anchors are synchronized and the target node clock runs freely. It jointly estimates the clock skew, the clock offset and the position of the target node. Furthermore, it considers the uncertainties of the anchor clocks and positions, and formulates a generalized total least-squares problem to cope with these uncertainties. However, it is a big challenge to first synchronize all the anchors.

In this paper, we propose a robust time-based localization method with the help of anchors for asynchronous networks with clock offsets, which subsumes the localization method proposed in [15] as a special case. UWB-IRs are employed for high resolution TOA ranging. Moreover, low duty cycle, low probability of detection and speed of light transmission make an UWB-IR ideal for secure communication and localization. The TWR protocol is facilitated by UWB ranging. However, this TWR protocol is vulnerable to a misbehavior of deceitful target nodes, which send fraudulent timestamps to spoof their processing time [16]. Furthermore, target nodes may submit inaccurate timestamps due to their asynchronous clocks or other reasons. Thus, the current protocol is not efficient and even fails under those circumstances. The reliability of timestamps in the time-based localization has to be taken into account.

We employ the asymmetric trip ranging (ATR) protocol proposed in [17] to facilitate clock offset cancellation. Moreover, the ATR protocol takes advantage of the broadcast property of WSNs and reduces the communication load. All the anchors can obtain ranging information in one ranging procedure. By ignoring the processing time report from the target node, we estimate the target position based on the timestamps from the anchors. As a result, the fact that the target node is not synchronized to the anchors does not have any influence on our method. Closed-form least-squares (LS) and weighted LS estimators are derived to accurately estimate the target node

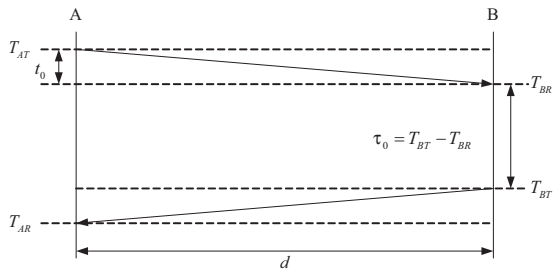

Fig. 1. An example of the two-way ranging protocol.

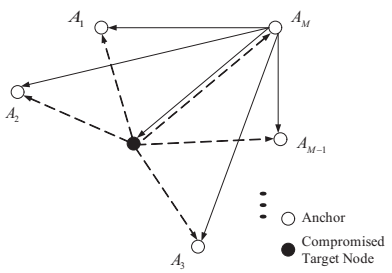

Fig. 2. An example of the ATR protocol.

position. Moreover, Cramér-Rao Bounds (CRBs) are derived as a benchmark.

The rest of the paper is organized as follows. In Section II, we review the TWR protocol. The system model is given in Section III. The robust localization algorithm is proposed in Section IV. Performance bounds and simulation results are shown in Section V. The conclusions are drawn at the end of this paper.

II. The two-way ranging protocol

The TWR protocol used in the IEEE 802.15.4a standard [14] facilitates ranging between two nodes. The packet structure proposed by the standard is composed of a synchronization header (SHR) preamble, a physical layer header (PHR) and a data field. The first pulse of the PHR is called the ranging marker (RMARKER). The moment when the RMARKER leaves or arrives at the antenna of a node is critical to ranging. An example of the TWR protocol is shown in Fig. 1. Node A (or Node B) records T_{AT} (or T_{BT}) and T_{AR} (or T_{BR}) upon the departure and the arrival of the RMARKER, respectively. Thus, the time of flight (TOF) t_0, which is linear to the distance d (the ranging target) between node A and node B ($d = ct_0$, where c is the speed of light), is given by

$$t_0 \;=\; \frac{1}{2}\left(\frac{T_{AR}-T_{AT}}{\alpha_A}-\frac{\tau_0}{\alpha_B}\right)+n, \qquad (1)$$

where $\tau_0 = T_{BT} - T_{BR}$ is the processing time at node B, α_A and α_B are the clock skews of node A and node B, respectively, and n is the aggregate error term. As the differences of the timestamps are employed in (1), the clock offsets are canceled. The aggregate error term n in (1) counts for the leading edge detection (LED) errors [14], which are due to the detection of the first multipath component of the received RMARKER, and the uncertainties of the internal propagation paths [14], which are caused by the difficulties to measure the events exactly at the antenna. Moreover, n can also contain communication and quantization errors.

Let us now focus on the robustness of the TWR protocol. According to (1), the TOF t_0 depends not only on the timestamps T_{AR} and T_{AT} at node A, but also on the processing time τ_0 at node B. The dependence on the reliability and synchronization of two different nodes is a weak point of the TWR protocol. Thus, the TWR protocol is vulnerable to the node misbehavior. For example, assume node B is compromised and tries to cheat node A about its distance by tampering its processing time as τ_0'. Then, t_0 will be miscalculated, since node A is not aware of the misbehavior of node B. In the following, we adopt the same packet structure as in the standard and employ the ATR protocol to overcome the shortcomings of the TWR protocol.

III. System Model of Asynchronous Networks with Clock offsets

Considering M anchor nodes and one target node, we would like to estimate the position of the target node. Our method can also be extended to multiple target nodes. Moreover, located target nodes can be viewed as new anchors that can facilitate the localization of other target nodes. All the nodes are distributed in an l-dimensional space, e.g., $l = 2$ (a plane) or $l = 3$ (a space). The coordinates of the anchor nodes are known and defined as $\mathbf{X}_a = [\mathbf{x}_1\ \mathbf{x}_2 \ldots\ \mathbf{x}_M]_{l\times M}$, where the vector $\mathbf{x}_i = [x_{1,i}\ x_{2,i}\ \ldots\ x_{l,i}]^T$ indicates the known coordinates of the ith anchor node. We employ a vector $\mathbf{x}$ of length l to denote the unknown coordinates of the target node. In asynchronous networks with clock offsets, the target node clock runs freely, and the clock skews of all the anchors are equal to 1 or treated as 1. There are only clock offsets among all the anchors. The timing relation between the ith anchor clock $C_i(t)$ and the absolute time t can be described as [7] $C_i(t) = t + \theta_i, i = 1, \ldots, M$, where θ_i is the unknown clock offset of $C_i(t)$ relative to the absolute clock. Moreover, the model for the target clock is given by $C_s(t) = \alpha_s t + \theta_s$, where α_s and θ_s denote the unknown clock skew and clock offset of the target node clock relative to the absolute clock.

To make full use of the broadcast property of wireless signals, we employ the ATR protocol proposed in [17] shown in Fig. 2. The ATR protocol makes all the other anchors listen to the ranging packets and record timestamps locally, when one anchor and the target node exchange their ranging packets. It can obtain more information than the TWR protocol, where all the other nodes are idle, when two nodes exchange their ranging packets. The ATR protocol starts with one of the anchors initiating the ranging request and recording a timestamp when its RMARKER departures, which can also be interpreted as the time when that anchor receives its own RMARKER without any delay. Without loss of generality, we assume the Mth anchor initiates the ranging request, and we denote the time recorded at the Mth anchor as T_{MR}. Consequently, all the

other anchors and the target node receive the ranging request and record their own timestamps $T_{iR},\ i=1,\ldots,M-1$ and T_{SR} respectively, as soon as they detect the RMARKER from the Mth anchor. The target node processes the ranging request and broadcasts a response. The departure time of the target RMARKER is recorded as T_{ST}. Define $\tau = T_{ST} - T_{SR}$ as the true processing time of the target node. Each anchor in the network detects the broadcast ranging response from the target node, and records its own timestamp for the arrival of the target RMARKER as $T_{iS},\ i=1,\ldots,M$. If a compromised target node tampers its processing time as τ', or a target node reports τ' due to the clock skew or the internal delay, all the distance measurements would be decreased or enlarged by $c|\tau-\tau'|$ (where c is the speed of light), which would lead to a meaningless position estimate.

For the ith anchor node, the difference between T_{iS} and T_{iR} relates to the distance as

$$\begin{aligned} c(T_{iS}-T_{iR}) &= d_i + d_M + \Delta - d_{iM} + n_{iS} - n_{iR}, \\ & \quad i=1,2,\ldots,M, \end{aligned} \tag{2}$$

where $d_i = \|\mathbf{x}_i - \mathbf{x}\| = \sqrt{\|\mathbf{x}_i\|^2 - 2\mathbf{x}_i^T\mathbf{x} + \|\mathbf{x}\|^2}$ is the unknown distance between the ith anchor and the target node, $\Delta = c\tau$ is the unknown distance corresponding to the target node processing time, and $d_{iM} = \|\mathbf{x}_i - \mathbf{x}_M\|$ is the known distance between the ith and the Mth anchors. Furthermore, n_{iS} and n_{iR} denote the distance errors translated from the measurement errors of T_{iS} and T_{iR}, respectively, which are aggregate error terms as we have discussed in Section II. Note that the recordings of T_{iS} and $T_{iR},\ i=1,\ldots,M-1$ are triggered by the received RMARKERs, and thus the same internal delays are involved, which are canceled out by making differences of timestamps recorded at the same node as indicated in (2). By making these differences, the clock offsets at the anchors can also be canceled[1]. The situation is different for the Mth anchor, since it records T_{MR} and T_{MS} upon transmitting and receiving the RMARKERs, respectively. As a result, the internal delays of the transmission path and the receiving path are added up when computing $T_{MS}-T_{MR}$. Thus, we assume that the main part of the Mth anchor's internal delay is compensated beforehand as accomplished in [12]. But different from [12], compensation is not required for the other anchors in our scheme. Consequentially, n_{iS} and n_{iR} can be modeled as zero mean random variables with variance σ_{iS}^2 and σ_{iR}^2, respectively [13]. Defining $\mathbf{u} = c[T_{1S},\ T_{2S},\ \ldots,\ T_{MS}]^T$, $\mathbf{v} = c[T_{1R},\ T_{2R},\ \ldots,\ T_{MR}]^T$, $\mathbf{d} = [d_1,\ d_2,\ \ldots,\ d_M]^T$, $\mathbf{d}_a = [d_{1M},\ d_{2M},\ \ldots,\ d_{(M-1)M},\ 0]^T$, $\mathbf{n}_s = [n_{1S},\ n_{2S},\ \ldots,\ n_{MS}]^T$ and $\mathbf{n}_r = [n_{1R},\ n_{2R},\ \ldots,\ n_{(M-1)R},\ n_{MR}]^T$, we can write (2) in vector form as

$$\mathbf{u} - \mathbf{v} = \mathbf{d} + (d_M + \Delta)\mathbf{1}_M - \mathbf{d}_a + \mathbf{n}_s - \mathbf{n}_r. \tag{3}$$

In order to be immune to a misbehavior of the compromised target node or to incorrect timestamps due to the randomness of the target node clock, we do not employ the timestamp report from the target node, but only use it as a trigger at each anchor. We estimate the target position only based on the timestamps T_{iR} and $T_{iS}, i=1,\ldots,M$, recorded locally at the M anchors. Because we do not use the timestamps of the target node, its clock parameters, such as clock skew, clock offset and internal delay, do not have any impact on our scheme. This distinguishes our algorithm from others that use the timestamps of the target node, such as [9], [12], [13]. It is easy for the target node to cheat one anchor, but it is almost impossible to cheat all the anchors simultaneously. We remark that the cooperative positioning protocol proposed in [18] is similar to our ATR protocol. However, our method differs from [18] in several aspects: (i) we do not use the timestamps from the target node, and thus our method is more robust to unreliable timestamps; (ii) the target node processing time is unknown; and (iii) we propose low complexity closed-form solutions for localization, instead of complex MLEs.

IV. Robust Localization Algorithm

Since we do not use the timestamps from the target node, the clock parameters of the target node do not impact its position estimate. More specifically, we treat Δ (the distance corresponding to the target node processing time) in (3) as an unknown parameter. Note that (3) is a linear equation with respect to (w.r.t.) Δ, but it is a complicated nonlinear equation w.r.t. $\mathbf{x}$ due to d_M and $\mathbf{d}$. We are not interested in methods with a high computational complexity, such as the MLE which also requires the unknown noise pdf. Because of the low cost and low power constraints of a WSN, we explore low-complexity closed-form solutions for localization.

Since $\Delta \gg d_i$, Δ is a dominant term at the right hand side of (3). In order to extract useful distance information, we have to preprocess (3). Instead of choosing a reference anchor node as proposed in [15], we employ an orthogonal projection $\mathbf{P}$ onto the orthogonal complement of $\mathbf{1}_M$, which is given by $\mathbf{P} = \mathbf{I}_M - \frac{1}{M}\mathbf{1}_M\mathbf{1}_M^T$. Since $\mathbf{P}\mathbf{1}_M = \mathbf{0}_M$, $\mathbf{P}$ can be used to eliminate the term $(d_M+\Delta)\mathbf{1}_M$ in (3). As a result, premultiplying both sides of (3) with $\mathbf{P}$, we obtain

$$\mathbf{P}(\mathbf{u}-\mathbf{v}) = \mathbf{P}\mathbf{d} - \mathbf{P}\mathbf{d}_a + \mathbf{P}(\mathbf{n}_s - \mathbf{n}_r). \tag{7}$$

Note that $\mathbf{P}\mathbf{d} = \mathbf{d} - \bar{d}\mathbf{1}_M$, where $\bar{d} = \frac{1}{M}\sum_{i=1}^M d_i$ is the unknown average of the distances between the target node and the anchors. Thus, (7) can be rewritten as

$$\mathbf{P}(\mathbf{u}-\mathbf{v}) = \mathbf{d} - \bar{d}\mathbf{1}_M + \mathbf{P}\mathbf{d}_a + \mathbf{P}\mathbf{n}_s - \mathbf{P}\mathbf{n}_r. \tag{8}$$

Keeping $\mathbf{d}$ on one side, moving the other terms to the other side, and making an element-wise multiplication, we achieve

$$\begin{aligned} \boldsymbol{\psi}_a - 2\mathbf{X}_a^T\mathbf{x} + \|\mathbf{x}\|^2\mathbf{1}_M = (\mathbf{P}(\mathbf{u}-\mathbf{v}+\mathbf{d}_a)) \odot (\mathbf{P}(\mathbf{u}-\mathbf{v}+\mathbf{d}_a)) \\ + \bar{d}^2\mathbf{1}_M + 2\bar{d}\mathbf{P}(\mathbf{u}-\mathbf{v}+\mathbf{d}_a) + \mathbf{n}_{rs}, \end{aligned} \tag{9}$$

where $\boldsymbol{\psi}_a = [\|\mathbf{x}_1\|^2,\ \|\mathbf{x}_2\|^2,\ \ldots,\ \|\mathbf{x}_M\|^2]^T$, and

$$\mathbf{n}_{rs} = -(\mathbf{P}(\mathbf{n}_s-\mathbf{n}_r)) \odot (\mathbf{P}(\mathbf{n}_s-\mathbf{n}_r)) - 2\mathbf{d} \odot \mathbf{P}(\mathbf{n}_s-\mathbf{n}_r). \tag{10}$$

Defining $\mathbf{P}\mathbf{n}_r = \mathbf{n}_r - \bar{n}_r\mathbf{1}_M$ and $\mathbf{P}\mathbf{n}_s = \mathbf{n}_s - \bar{n}_s\mathbf{1}_M$, where $\bar{n}_r = \frac{1}{M}\sum_{i=1}^M n_{iR}$ and $\bar{n}_s = \frac{1}{M}\sum_{i=1}^M n_{iS}$, we can write the

[1]Note that this is different from the traditional TDOA approach, which requires synchronization among anchor nodes [3].

$$[\mathbf{n}_{rs}]_i = 2d_i(n_{iR}-\bar{n}_r-n_{iS}+\bar{n}_s)-(n_{iR}-\bar{n}_r-n_{iS}+\bar{n}_s)^2, \quad i=1,2,\ldots,M. \tag{13}$$

$$E[[\mathbf{n}_{rs}]_i] = \frac{2-M}{M}(\sigma_{iR}^2+\sigma_{iS}^2)-\frac{1}{M^2}\sum_{k=1}^{M}(\sigma_{kR}^2+\sigma_{kS}^2)\approx 0, \tag{14}$$

$$[\mathbf{\Sigma}_{rs}]_{i,j} = E[[\mathbf{n}_{rs}]_i[\mathbf{n}_{rs}]_j] \approx \begin{cases} 4d_i^2\left(\frac{M-2}{M}(\sigma_{iR}^2+\sigma_{iS}^2)+\frac{1}{M^2}\sum_{k=1}^{M}(\sigma_{kR}^2+\sigma_{kS}^2)\right), & i=j \\ 4d_id_j\left(\frac{1}{M^2}\sum_{k=1}^{M}(\sigma_{kS}^2+\sigma_{kR}^2)-\frac{1}{M}(\sigma_{iS}^2+\sigma_{jS}^2+\sigma_{iR}^2+\sigma_{jR}^2)\right), & i\neq j \end{cases}, \tag{15}$$

entries of $\mathbf{n}_{rs}$ as in (13) on the top of this page. Recall that $E[n_{iS}]=0$, $E[n_{iS}^2]=\sigma_{iS}^2$ and $E[n_{iS}n_{jS}]=0, i\neq j$, leading to $E[\bar{n}_s]=0$, $E[\bar{n}_s^2]=\frac{1}{M^2}\sum_{i=1}^{M}\sigma_{iS}^2$ and $E[\bar{n}_s n_{iS}]=\frac{1}{M}\sigma_{iS}^2$. The stochastic properties of n_{iR} can be obtained in a similar way. Moreover, n_{iS} and $n_{iR}, i=1,\ldots,M$ are uncorrelated. As a result, the stochastic properties of $\mathbf{n}_{rs}$ are given by (14) and (15) on the top of this page, where we ignore the higher order noise terms to obtain (15) and assume $E[[\mathbf{n}_{rs}]_i]\approx 0$ under the condition of sufficiently small measurement errors. Note that the noise covariance matrix $\mathbf{\Sigma}_{rs}$ depends on the unknown $\mathbf{d}$.

As (9) is still a nonlinear equation w.r.t. $\mathbf{x}$, we make again use of the orthogonal projection $\mathbf{P}$ to eliminate the terms $\|\mathbf{x}\|^2$ and $\bar{d}^2$ in (9). By premultiplying both sides of (9) with $\mathbf{P}$ followed by rearranging, we arrive at

$$\begin{aligned} &\mathbf{P}\boldsymbol{\psi}_a-\mathbf{P}((\mathbf{P}(\mathbf{u}-\mathbf{v}+\mathbf{d}_a))\odot(\mathbf{P}(\mathbf{u}-\mathbf{v}+\mathbf{d}_a))) \\ =\ & 2\mathbf{P}\mathbf{X}_a^T\mathbf{x}+2\bar{d}\mathbf{P}(\mathbf{u}-\mathbf{v}+\mathbf{d}_a)+\mathbf{P}\mathbf{n}_{rs}. \end{aligned} \tag{11}$$

As a result, (11) becomes a linear equation w.r.t. both $\mathbf{x}$ and $\bar{d}$. Defining $\mathbf{b}=\boldsymbol{\psi}_a-((\mathbf{P}(\mathbf{u}-\mathbf{v}+\mathbf{d}_a))\odot(\mathbf{P}(\mathbf{u}-\mathbf{v}+\mathbf{d}_a)))$, $\mathbf{A}=2\left[\mathbf{X}_a^T,\ \mathbf{P}(\mathbf{u}-\mathbf{v}+\mathbf{d}_a)\right]$, and $\mathbf{y}=[\mathbf{x}^T,\ \bar{d}]^T$, we can finally rewrite (11) as

$$\mathbf{P}\mathbf{b} = \mathbf{P}\mathbf{A}\mathbf{y}+\mathbf{P}\mathbf{n}_{rs}. \tag{12}$$

We can find the LS and WLS solutions for (12) as

$$\hat{\mathbf{y}} = (\mathbf{A}^T\mathbf{P}\mathbf{A})^{-1}\mathbf{A}^T\mathbf{P}\mathbf{b}, \tag{13}$$

and

$$\hat{\mathbf{y}} = (\mathbf{A}^T\mathbf{P}\mathbf{W}\mathbf{P}\mathbf{A})^{-1}\mathbf{A}^T\mathbf{P}\mathbf{W}\mathbf{P}\mathbf{b}, \tag{14}$$

respectively, where $\mathbf{W}$ is a weighting matrix. The optimal weighting matrix $\mathbf{W}_o$ is given by

$$\mathbf{W}_o = (\mathbf{P}\mathbf{\Sigma}_{rs}\mathbf{P})^{\dagger}, \tag{15}$$

where we use the pseudo inverse because the $M\times M$ projection matrix $\mathbf{P}$ has rank $M-1$. Furthermore, $\mathbf{PA}$ should be a full rank tall matrix. Thus, the number of anchors M should be no less than $l+3$, which indicates that we need at least five anchors to estimate the target position on a plane. Since $\mathbf{W}_o$ depends on the unknown $\mathbf{d}$, we can update it iteratively. Consequently, the iterative WLS is summarized as follows

1) Initialize $\mathbf{W}$ using the estimate of $\mathbf{d}$ based on the LS estimate of $\mathbf{x}$;
2) Estimate $\hat{\mathbf{y}}$ using (14);
3) Construct $\mathbf{W}$ using (15), where $\mathbf{\Sigma}_{rs}$ is computed using $\hat{\mathbf{y}}$;
4) Repeat Steps 2) and 3) until no obvious improvement of the cost function $(\mathbf{b}-\mathbf{A}\mathbf{y})^T\mathbf{P}\mathbf{W}\mathbf{P}(\mathbf{b}-\mathbf{A}\mathbf{y})$ is observed.

An estimate of $\mathbf{x}$ is finally given by

$$\hat{\mathbf{x}} = [\mathbf{I}_l \quad \mathbf{0}_l]\hat{\mathbf{y}}. \tag{16}$$

We remark that the estimator (13) (or (14)) is equivalent to the unconstrained LS (or WLS) estimator to obtain $\mathbf{x}$, $\bar{d}$ and $\bar{d}^2-\|\mathbf{x}\|^2$ all together as discussed in [6]. We may even improve the estimation performance by exploring the relations among $\mathbf{x}$, $\bar{d}$ and $\bar{d}^2-\|\mathbf{x}\|^2$ as constraints. Constrained LS (CLS) and weighted CLS estimators can be derived as in [5]. However, it is extremely difficult to take the relation between $\mathbf{x}$ and $\bar{d}$ into account, since it is highly non-linear.

The distance Δ corresponding to the target node processing time can be estimated as

$$\hat{\Delta} = \mathbf{1}_M^T(\mathbf{u}-\mathbf{v}-\hat{\mathbf{d}}+\mathbf{d}_a)-\hat{d}_M, \tag{17}$$

where $\hat{d}_i=\|\hat{\mathbf{x}}-\mathbf{x}_i\|,\ i=1,\ldots,M$ are the distance estimates between the target node and the anchors based on $\hat{\mathbf{x}}$. We remark that there are mathematical similarities between our data model (3) and the data model in [12], if we regard $d_M+\Delta$ in (3) as an unknown internal delay. However, we employ a novel ATR protocol and estimate the parameters in a different way.

V. Performance Bounds and Numerical Examples

As a well-adopted lower bound, the Cramèr-Rao bound (CRB) based on the model (3) in Section III is derived in Appendix B. Here, we exemplify the CRB for location estimation on a plane, e.g. we take $l=2$. Let us define $\boldsymbol{\theta}=[\Delta,\ \mathbf{x}^T]^T$, where $\mathbf{x}=[x_1,\ x_2]^T$. The inverse of the fisher information matrix (FIM) $\mathbf{I}(\boldsymbol{\theta})$ is then given by

$$\mathbf{I}^{-1}(\boldsymbol{\theta}) = \begin{bmatrix} \frac{1}{f} & -\frac{1}{f}\mathbf{r}^T\mathbf{G}^{-1} \\ -\frac{1}{f}\mathbf{G}^{-1}\mathbf{r} & \left(\mathbf{G}-\frac{1}{k}\mathbf{r}\mathbf{r}^T\right)^{-1} \end{bmatrix}, \tag{18}$$

where $f=k-\mathbf{r}^T\mathbf{G}^{-1}\mathbf{r}$, with k, $\mathbf{r}$, and $\mathbf{G}$ defined in Appendix B. Consequently, we obtain $\mathrm{CRB}(x_1)=[\mathbf{I}^{-1}(\boldsymbol{\theta})]_{2,2}$ and $\mathrm{CRB}(x_2)=[\mathbf{I}^{-1}(\boldsymbol{\theta})]_{3,3}$. We observe that Δ is not part of $\mathbf{I}^{-1}(\boldsymbol{\theta})$. Therefore, no matter how large Δ, it has the same influence on the CRB.

Let us now evaluate the performance of the proposed robust localization algorithm by Monte Carlo simulations, and compare it with the CRB. We consider two simulation setups: Setup 1 and Setup 2. In Setup 1, the anchors are evenly

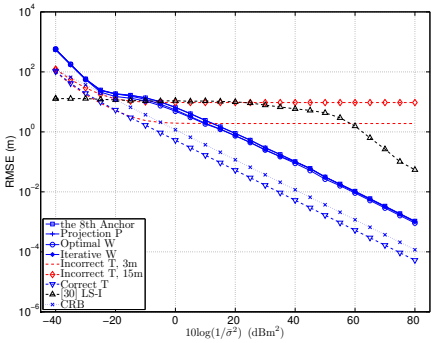

(a) Setup 1, $M = 8$

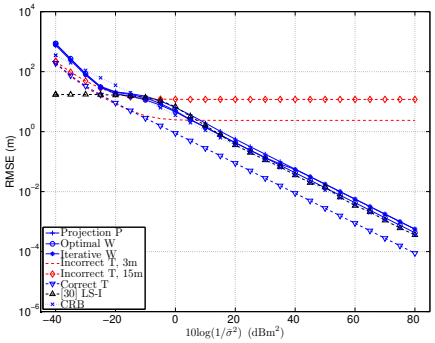

(b) Setup 2, $M = 8$

Fig. 3. RMSE of $\mathbf{x}$ for asynchronous networks with clock offsets

located on the edges of a $40\,\mathrm{m} \times 40\,\mathrm{m}$ rectangular to mimic an indoor geometry scale. Meanwhile the target node is randomly located on a grid with cells of size $1\,\mathrm{m} \times 1\,\mathrm{m}$ inside the rectangular. In Setup 2, all anchors and the target node are randomly distributed on the grid inside the rectangular. Due to the broadcast property of the ranging protocol, we assume that σ_{iS}^2 and σ_{iR}^2 are related to the distances according to the path loss law. Thus we define the average noise power as $\bar{\sigma}^2 = 1/M \sum_{i=1}^{M} \sigma_{iS}^2$, where σ_{iR}^2 and σ_{iS}^2 are chosen to fulfill the condition that all σ_{iR}^2/d_{iM}^2 and σ_{iS}^2/d_i^2 are equal as in [5]. Note that since $d_{MM} = 0$, we simply assume $\sigma_{MR}^2 = 0$ and $n_{MR} = 0$. The processing time of the target node is 5 ms, and as a result the corresponding distance Δ is $3\times10^8\times5\times10^{-3} = 1.5\times10^6$ m. The performance criterion is the root mean square error (RMSE) of $\hat{\mathbf{x}}$ vs. SNR, which can be expressed as $\sqrt{1/N_{exp}\sum_{j=1}^{N_{exp}} \|\hat{\mathbf{x}}^{(j)} - \mathbf{x}\|^2}$, where $\hat{\mathbf{x}}^{(j)}$ is the estimate obtained in the jth trial. Each simulation result is averaged over $N_{exp} = 1000$ Monte Carlo trials. We would like to compare our localization algorithm with the conventional localization algorithm using the TWR protocol, which is clarified in Appendix A, and the algorithm LS-I in [13]. We assume that the algorithm LS-I in [13] is employed with accurate knowledge of the anchor clock parameters and positions. The number of rounds of two-way message exchanges is four, as with more than four rounds, the estimation performance improvement is only marginal [13]. The clock offset and the clock skew of the target is randomly generated in the range of $[1\text{ns}, 10\text{ns}]$ and $[1 - 100\,\text{ppm}, 1 + 100\,\text{ppm}]$, respectively.

Fig. 3(a) and Fig. 3(b) show the localization performance of respectively Setup 1 and Setup 2 with eight anchors with clock offsets. In each Monte Carlo run, we generate a new geometry. In both figures, the dashed lines with no and "$\diamondsuit$" markers represent the conventional localization algorithm using the fraudulent timestamp report from the target node with 3 m and 15 m errors, respectively. According to the figures, they cannot estimate the target position correctly even with sufficiently small noise terms. A larger timestamp error introduces a higher error floor. The dashed line with $\bigtriangledown$ markers illuminates the conventional localization algorithm using the correct timestamp report. It is slightly better than the CRB of our method for Setup 1 (the dotted line with $\times$ markers), but much better than the one for Setup 2. This is reasonable, since the conventional method estimates less parameters than the proposed method. The performance of the algorithm LS-I (the dashed line with $\bigtriangleup$ markers) in Setup 1 and Setup 2 is quite different. It is worse than our method in Section IV (the solid lines with different markers) in Setup 1, whereas better than our method in Setup 2. The algorithm LS-I seems to be sensitive to geometries, where the target node is inside the region restricted by the anchors. Moreover, $8M$ ranging packets are transmitted in the algorithm LS-I compared to only 2 ranging packets in our scheme, so our communication load is much less. Furthermore, the method in Section IV is immune to a fraudulent timestamp report and robust to the randomness of the target node clock, and its localization performance is accurate with sufficiently small noise terms. The solid line with "$\square$" markers shows the performance of the LS estimator using the eighth anchor as the reference node [15], whereas the solid line with "$+$" markers indicates the performance of our proposed LS estimator using the projection $\mathbf{P}$. Note that they almost overlap. The solid lines with "$\circ$" and "$*$" markers denote the performance of our proposed WLS method with an optimal weighting and iterative weighting matrix, respectively. The fact that they almost overlap indicates that if we use the LS estimate as an initial point, the iterative WLS can converge to the WLS with optimal weighting. The performance of the WLS with optimal weighting is slightly better than LS and the iterative WLS estimators. Considering the computational complexity and the performance, the LS estimator would be the best option.

VI. Conclusions

In this work, we propose a robust localization strategy based on TOA measurements for asynchronous networks with clock offsets. Regardless of the honesty of the timestamps from the target node, we employ a novel ATR protocol, which leads to a localization method that is robust to uncertainties of the target node. Furthermore, closed-form LS and WLS estimators are derived to accurately estimate the target position.

Appendix A
Conventional localization by the TWR protocol

Assume the distances between the target and the anchor nodes are measured by executing the TWR protocol. For

$$p(\mathbf{u};\boldsymbol{\theta}) = \frac{1}{\sqrt{(2\pi)^M \prod_{i=1}^{M}(\sigma_{iS}^2+\sigma_{iR}^2)}} \exp\left(-\sum_{i=1}^{M}\frac{1}{2(\sigma_{iS}^2+\sigma_{iR}^2)}(u_i - v_i - d_i - d_M + d_{iM} - \Delta)^2\right). \quad (22)$$

$$\mathbf{Q} = \begin{bmatrix} \sum_{i=1}^{M}\frac{1}{\sigma_{iS}^2+\sigma_{iR}^2}\left(\frac{x_1-x_{1,i}}{\|\mathbf{x}-\mathbf{x}_i\|}+\frac{x_1-x_{1,M}}{\|\mathbf{x}-\mathbf{x}_M\|}\right)^2 & \sum_{i=1}^{M}\frac{1}{\sigma_{iS}^2+\sigma_{iR}^2}\left(\frac{x_1-x_{1,i}}{\|\mathbf{x}-\mathbf{x}_i\|}+\frac{x_1-x_{1,M}}{\|\mathbf{x}-\mathbf{x}_M\|}\right)\left(\frac{x_2-x_{2,i}}{\|\mathbf{x}-\mathbf{x}_i\|}+\frac{x_2-x_{2,M}}{\|\mathbf{x}-\mathbf{x}_M\|}\right) \\ \sum_{i=1}^{M}\frac{1}{\sigma_{iS}^2+\sigma_{iR}^2}\left(\frac{x_2-x_{2,i}}{\|\mathbf{x}-\mathbf{x}_i\|}+\frac{x_2-x_{2,M}}{\|\mathbf{x}-\mathbf{x}_M\|}\right)\left(\frac{x_1-x_{1,i}}{\|\mathbf{x}-\mathbf{x}_i\|}+\frac{x_1-x_{1,M}}{\|\mathbf{x}-\mathbf{x}_M\|}\right) & \sum_{i=1}^{M}\frac{1}{\sigma_{iS}^2+\sigma_{iR}^2}\left(\frac{x_2-x_{2,i}}{\|\mathbf{x}-\mathbf{x}_i\|}+\frac{x_2-x_{2,M}}{\|\mathbf{x}-\mathbf{x}_M\|}\right)^2 \end{bmatrix}, \quad (23)$$

$$\mathbf{r} = \left[\sum_{i=1}^{M}\frac{1}{\sigma_{iS}^2+\sigma_{iR}^2}\left(\frac{x_1-x_{1,i}}{\|\mathbf{x}-\mathbf{x}_i\|}+\frac{x_1-x_{1,M}}{\|\mathbf{x}-\mathbf{x}_M\|}\right) \quad \sum_{i=1}^{M}\frac{1}{\sigma_{iS}^2+\sigma_{iR}^2}\left(\frac{x_2-x_{2,i}}{\|\mathbf{x}-\mathbf{x}_i\|}+\frac{x_2-x_{2,M}}{\|\mathbf{x}-\mathbf{x}_M\|}\right)\right]^T. \quad (24)$$

each execution, we obtain four timestamps, namely T_{iS} and T_{iT} (the time when the RMARKER leaves the anchors) at the ith anchor, and $T_{ST}^{(i)}$ and $T_{SR}^{(i)}$ at the target. Recalling the parameters defined in the previous sections, the relations between the timestamps are described as follows

$$c(T_{iS} - T_{iT}) = 2d_i + \Delta + n_{iS} - n_{iT}, \quad (22)$$
$$c(T_{ST}^{(i)} - T_{SR}^{(i)}) = \Delta + n_{ST}^{(i)} - n_{SR}^{(i)}, \quad (23)$$

where we assume exact knowledge of the time when the RMARKER leaves, thus $n_{iT} = n_{ST}^{(i)} = 0$, and $n_{SR}^{(i)}$ is a zero mean random variable with the same variance σ_{iS}^2 as n_{iS}. We first obtain an estimate of Δ based on (23), thus $\hat{\Delta} = \frac{1}{M}\sum_{i=1}^{M} c(T_{ST}^{(i)} - T_{SR}^{(i)})$. Plugging $\hat{\Delta}$ into (22), we write (22) in vector form without noise terms as

$$\mathbf{u} - \mathbf{w} = 2\mathbf{d} + \hat{\Delta}\mathbf{1}_M, \quad (24)$$

where $\mathbf{w} = [T_{1T} \quad T_{2T} \quad \dots \quad T_{MT}]^T$. The target position can now be estimated based on (24) using the same LS estimator as in Section IV.

APPENDIX B
CRB DERIVATION

We analyze the CRB for jointly estimating Δ and $\mathbf{x}$ based on (9). The FIM $\mathbf{I}(\boldsymbol{\theta})$ is employed, with entries defined as:

$$[\mathbf{I}(\boldsymbol{\theta})]_{ij} = -E\left[\frac{\partial^2}{\partial\theta_i\partial\theta_j}\ln p(\mathbf{u};\boldsymbol{\theta})\right], \quad (25)$$

where $p(\mathbf{u};\boldsymbol{\theta})$ is shown in (22) on the top of this page. In the case of localization on a plane ($l = 2$), $\mathbf{I}(\boldsymbol{\theta})$ can be specified as

$$\mathbf{I}(\boldsymbol{\theta}) = \begin{bmatrix} k & \mathbf{r}^T \\ \mathbf{r} & \mathbf{Q} \end{bmatrix}, \quad (26)$$

where $k = \sum_{i=1}^{M}\frac{1}{\sigma_{iS}^2+\sigma_{iR}^2}$, and where $\mathbf{Q}$ and $\mathbf{r}$ are defined in (23) and (24) on the top of this page, respectively.

REFERENCES

[1] I. Akyildiz, W. Su, Y. Sankarasubramaniam, and E. Cayirci, "A survey on sensor networks," *IEEE Commun. Mag.*, vol. 40, no. 8, pp. 102 – 114, Aug. 2002.

[2] S. Gezici, Z. Tian, G. Giannakis, H. Kobayashi, A. Molisch, H. Poor, and Z. Sahinoglu, "Localization via ultra-wideband radios: a look at positioning aspects for future sensor networks," *IEEE Signal Process. Mag.*, vol. 22, pp. 70–84, July 2005.

[3] A. Sayed, A. Tarighat, and N. Khajehnouri, "Network-based wireless location: challenges faced in developing techniques for accurate wireless location information," *IEEE Signal Process. Mag.*, vol. 22, no. 4, pp. 24–40, July 2005.

[4] A. Savvides, C.-C. Han, and M. B. Strivastava, "Dynamic fine-grained localization in ad-hoc networks of sensors," in *Proc. ACM MobiCom*, July 2001, pp. 166–179.

[5] K. Cheung, H. So, W.-K. Ma, and Y. Chan, "Least squares algorithms for time-of-arrival-based mobile location," *IEEE Trans. Signal Process.*, vol. 52, no. 4, pp. 1121 – 1130, Apr. 2004.

[6] P. Stoica and J. Li, "Lecture notes - source localization from range-difference measurements," *IEEE Signal Process. Mag.*, vol. 23, no. 6, pp. 63–66, Nov. 2006.

[7] B. Sundararaman, U. Buy, and A. Kshemkalyani, "Clock synchronization for wireless sensor networks: a survey," *Ad Hoc Networks*, vol. 3, no. 3, pp. 281 – 323, Jan. 2005.

[8] M. Rydstrom, E. Strom, and A. Svensson, "Clock-offset cancellation methods for positioning in asynchronous sensor networks," in *Proc. IEEE IWCMC*, vol. 2, June 2005, pp. 981–986.

[9] B. Denis, J.-B. Pierrot, and C. Abou-Rjeily, "Joint distributed synchronization and positioning in uwb ad hoc networks using TOA," *IEEE Trans. Microw. Theory Tech.*, vol. 54, no. 4, pp. 1896 – 1911, June 2006.

[10] T. Li, A. Ekpenyong, and Y.-F. Huang, "Source localization and tracking using distributed asynchronous sensors," *IEEE Trans. Signal Process.*, vol. 54, no. 10, pp. 3991 –4003, 2006.

[11] C. Yan and H. Fan, "Asynchronous self-localization of sensor networks with large clock drift," in *Proc. IEEE MobiQuitous*, Aug. 2007, pp. 1–8.

[12] K. Yu, Y. Guo, and M. Hedley, "TOA-based distributed localisation with unknown internal delays and clock frequency offsets in wireless sensor networks," *IET Signal Processing*, vol. 3, no. 2, pp. 106 –118, 2009.

[13] J. Zheng and Y.-C. Wu, "Joint time synchronization and localization of an unknown node in wireless sensor networks," *IEEE Trans. Signal Process.*, vol. 58, no. 3, pp. 1309 –1320, Mar. 2010.

[14] IEEE Working Group 802.15.4, "Part 15.4: Wireless medium access control (MAC) and physical layer (PHY) specifications for low-rate wireless personal area networks (WPANs)," Tech. Rep., 2007.

[15] Y. Wang, X. Ma, and G. Leus, "An UWB ranging-based localization strategy with internal attack immunity," in *Proc. IEEE ICUWB*, Sept. 2010.

[16] S. Capkun and J.-P. Hubaux, "Secure positioning of wireless devices with application to sensor networks," in *Proc. IEEE INFOCOM*, vol. 3, Mar. 2005, pp. 1917 – 1928.

[17] Y. Wang, G. Leus, and X. Ma, "Time-based localization for asynchronous wireless sensor networks," in *Proc. IEEE ICASSP*, Prague, Czech Republic, May 2011, accepted.

[18] Z. Sahinoglu and S. Gezici, "Enhanced position estimation via node cooperation," in *Proc. IEEE ICC*, May 2010, pp. 1 –6.